Microwave surface states in periodic microstripe

Aleksey A. Girich, Anna A. Kharchenko, Sergey I. Tarapov, Szymon Mieszczak, Jarosław W. Kłos, *Member, IEEE* , Maciej Krawczyk, *Member, IEEE*

***Abstract*— We have investigated the transmission of microwave signal trough the stepped impedance filter in the form of periodic microstripe. Such periodic structure can be considered as peculiar sort of the one-dimensional photonic crystal where the sequence of stop bands appears due to Bragg scattering of electromagnetic waves. It is known, that the modes (states) localized at the terminations (surfaces) of periodic structure can exist in stop bands of photonic crystals. For the considered microstripe filter we have looked for the existence of such microwave surface states. We have investigated how to tune their positions inside the stop band by adjusting the structural parameters of the microstripe. The work presents the results of measurements and numerical simulations of the transmission spectrum explained with the aid of the simple model based on the lumped element ladder filter. The results we obtained can be used in designing of microwave filers for frequency-division multiplexing, which allow to introduce the pilot signal of selected frequency in the form of surface state.**

***Index Terms*— Frequency domain, microstrip filters, periodic structures, photonic microwave filters**

I. Introduction

The periodically shaped microstripe transmission lines (MSTL) are used in microwave technology as so-called stepped-impedance filters [1-2]. Those structures can be considered as one-dimensional photonic crystals (PC) operating in GHz frequency range [3-5]. In PC the surfaces/boundaries are the defects which break the periodicity of the structure. The modes localized on defects (including surfaces [6,7] or interfaces [3-5,8-9]) can be observed at selected frequencies in the stop bands of PC, if the appropriate matching conditions are fulfilled [5,10]. The surface states are characterized by complex propagation constant (complex wave vector) and therefore they decay exponentially inside the periodic structure being localized on the surfaces.

The surface states can appear for different kind of periodic structures (electronic superlattices [11], magnonic crystals [12]) where the wave excitations of different nature are observed (elastic waves, spin waves). The existence of surface states depends both on the bulk parameters (sizes and shape of the units cell) and the surface parameters (describing how the periodic structure is terminated). By changing the bulk parameters we can design the band structure supporting the existence of surface states. The modification of the surface parameters can tune the frequency of surfaces states within the stop band

One of the simplest geometry in which the surface states, in the meaning described above, can be observed is the structure of periodic line. Such systems, confined in two dimensions allow the wave to propagate in one direction. The periodic line (waveguide) is terminated in two points – surfaces – being the endings of the first and last cell in the periodic chain. By adjusting the geometry of the first and last cell one can change the frequency of surface states within the stop band. In the absence of surface states, such geometrical changes can induce this kind of states close to the edge of stop band and then shift them gradually towards the center of stop band.

For the periodic line, symmetric with respect to the flipping of both endings, the surface states appear in pairs, at very close frequencies. Each of this mode occupies both surfaces at once. For one mode from this pair the temporal oscillations on both surfaces take place in-phase, for the other one – out-of-phase. Excitations on both surfaces are correlated to each other due to the leaked tails penetrating the interior of the periodic structure. The rate of exponential decay of those tails is defined by imaginary part of the propagation constants. The strong localization corresponds to the large value of this parameter, and the surface state is observed at the center of stop band. On contrary, the surface modes are weaker localized, if their frequencies are close to the edges of stop band, where the imaginary part of propagation constant tends to zero. The pair of surfaces modes of the frequencies close to the center of stop band are well separated in frequency domain from the bulk modes (which can be beneficial for the utilization), but such modes can be almost degenerate (which can make their detection difficult).

The properties of surface states described above are general and refer also to the microwave devices under investigation. In this paper we investigated experimentally and numerically the conditions of appearance of surface state in MSTL and used the arguments known in photonics to explain the properties of surface states observed in MSTL.

The proposed system is interesting, because of potential

"This work was supported by the European Union's Horizon 2020 research and innovation programme under the Marie Skłodowska-Curie grant agreement No 644348 (MagIC). J.W.K. would like to acknowledge the support of the Foundation of Alfried Krupp Kolleg Greifswald"

A.A. Girich, A.A. Kharchenko and S.I. Tarapov are with O. Ya. Usikov Institute for Radiophysics and Electronics NAS of Ukraine, Ac. Proskura str. 12, Kharkov, 61085, Ukraine (e-mail: girich82@gmail.com, ganna.kharchenko@gmail.com, tarapov@ire.kharkov.ua)

S. M, J. W. K. and M. K Authors are with the Faculty of Physics, Adam Mickiewicz University in Poznań, Umultowska 85, 61-614 Poznań, Poland, J.W.K is now visiting the Institute of Physics, Greiswald Univeristy, Felix-Hausdorff-Str. 6, 17489, Greifswald, Germany (e-mail: klos@amu.edu.pl, krawczyk@amu.edu.pl).

applications of periodic MSTL, where the localized modes are isolated in frequency domain from the bulk modes grouped in transmission bands. One can consider such MSTL as a bandpass filter for frequency-division multiplexing which allows to introduce the reference pilot signal as a surface state [13].

II. The system

The investigated system has a form of periodic MSTL (see Fig. 1(a,b)) composed of 5 cells (see Fig. 1(c,d)). Each internal (bulk) cell (Fig. 1(c)) consists the section of wider microstripe (w = 4 mm) of the length l = 10 mm linked to the neighboring cells by thinner sections (1.2 mm in width). The bulk cell length d is equal to 16 mm. The width w_0 and length l_0 of the wider segment in surface cells and its total length d_0 (Fig. 1(d)) can by different. For experimentally realized structure, the values of surface parameters: w_0 and l_0 are equal to 9 mm and 1.5 mm, respectively, and kept: $d_0 = d$. We studied also experimentally the system with unaltered surface cells, where $w_0 = w$, $l_0 = l$, and $d_0 = d$, for reference. The microstripe structure is made on a

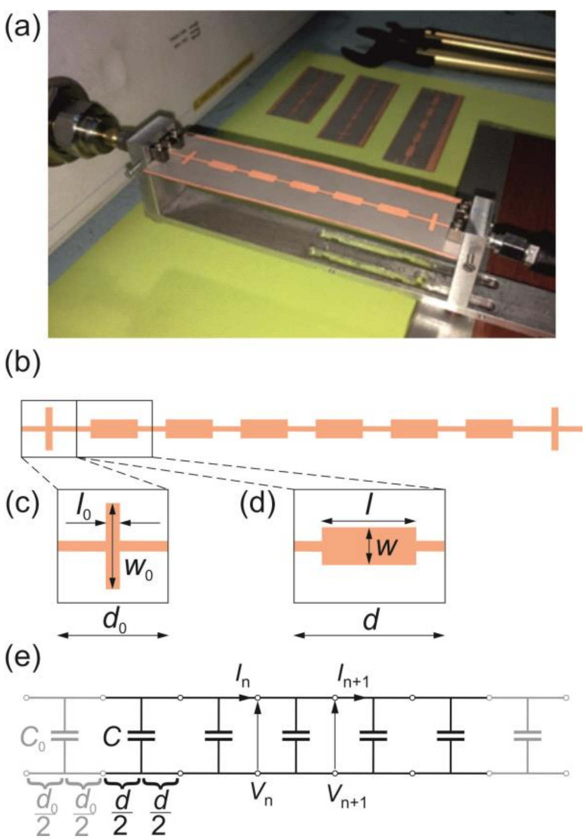

Fig.1. Periodic microstripe under investigation. (a) The photograph of experimental setup presenting the microstripe placed on the substrate. The bottom surface of the substrate is metalized and play the role of the ground plane. The input and output of the microstripe are connected to Network analyzer (NA5230) with standard 50Ω ports to measure S_{21} spectrum. (b) The geometry of the system. The line is composed of (c) n = 5 bulk cells and (d) two surface cells. The bulk and surface cells differ in the size: d, d_0, and in the geometrical parameters: (l,w), (l_0 ,w_0), describing the corrugation of the microstripe. (c) The simplified, one-dimensional model of periodic microstripe where the bulk and surface cell are represented by the symmetric two-port networks. Each network is composed of two phase-shifters (resulting from the acquiring of the phase at the distance d/2 or d_0/2 each) and shunt susceptance (resulting from the presence capacitance C or C_0, in each cell of the system).

substrate (Neltec) with dielectric constant ε = 2.2 + j 0.0012 and thickness t = 0.381 mm. For numerical studies we changed the surface parameters w_0 and l_0 continuously to induce surface states and to tune their frequencies. We used the simplified lumped element model (Fig. 1(e)) to explain the appearance of stop bands and surface states.

III. Model

We used Network Analyzer NA5230 to measure the transmission spectra (S_{21}). The S_{21} spectra was also extracted numerically. For numerical calculation of the transmission spectra and field distribution we used CST MICROWAVE STUDIO® software which is based on classical frequency domain calculation technique. To interpret the experimental and numerical outcomes, we introduced the model where the microstripe was replaced by equivalent lumped element system. We considered ladder multi-stop band filter being the cascade of symmetric two-terminal networks representing each cell of the MSTL (see Fig.1(e)). Each network is composed of shout capacitance and two phase shifters: one at input and the other one at output. The shout capacitance can be related to area of one cell of microstripe over the ground plate whereas the phase shift to its length. Each network can be then described by two parameters: the shunt capacitance C (C_0 for first and last network) and the length d (d_0 for the first and the last network). The shunt capacitance can be related to the geometry of the cell and dielectric constant of the substrate. The shunt capacitors formed by successive cells of microstripe are partially open and microwave propagate partially in air above MSTL. We introduced, in lumped-element model, the effective dielectric constant $\varepsilon_{\rm eff}$, lower then dielectric constant of the substrate: $\varepsilon_{\rm eff} < \varepsilon$. The other parameter, which has to be specified for lumped-elements model, is the characteristic impedance Z_C of MSTL. The impedance Z_C allows to relate electric and magnetic field in real MSTL to voltage an current in ladder filter.

The formal relation between output and input voltages and currents for elementary network (representing cell of MSTL) can be written with the aid of ABCD matrix [2]:

$$\begin{pmatrix} V_n \\ I_n \end{pmatrix} = \begin{pmatrix} A & B \\ C & D \end{pmatrix} \begin{pmatrix} V_{n+1} \\ I_{n+1} \end{pmatrix}. \qquad (1)$$

For our system the ABCD matrix $\boldsymbol{M}$ has a form [2]:

$$\begin{pmatrix} \cos(\Omega) - p\Omega \sin\Omega & j(p(\cos\Omega - 1) + \sin\Omega) \\ j(p(\cos\Omega + 1) + \sin\Omega) & \cos(\Omega) - p\Omega \sin\Omega \end{pmatrix} \qquad (2)$$

where $\Omega = k_0 d$ is dimensionless angular frequency. The parameter $k_0 = \omega / (c/\sqrt{\varepsilon_{\rm eff}})$ is the wave number in uniform space characterized by dielectric constant $\varepsilon_{\rm eff}$. The symbol p is defined as: $p = q\,(c/\sqrt{\varepsilon_{\rm eff}})\,(1/(2d))$ were $q = Z_C\,C$.

In infinite sequence of the networks, the voltages and currents are related to each other by propagation constant k_B:

$$V_n = e^{-jk_B d} V_{n+1}, \;\; I_n = e^{-jk_B d} I_{n+1}. \qquad (3)$$

The propagation constant k_B can be considered as Bloch wave number, known in physics for description of wave excitation in periodic systems [14]. The wave number k_B is real in the pass band and complex in the stop bands. Eqs. 1-3 allow to derive the dispersion relation which links the dimensionless frequency Ω (or wave number in uniform space: k_0) to dimensionless Bloch wave number $\theta_B = k_B\, d$.

$$\cos\theta_B = \cos\Omega - p\Omega\sin\Omega. \tag{4}$$

The lumped-elements model contains two parameters: ε_{eff} and p which are related in complex way to the parameters of real MSTL. In order to refer the model to real structure we fit the values of ε_{eff} and p to obtain the same ranges of pass and stop bands as these obtained from experimental and numerical studies. Then, having the values of ε_{eff} and p fixed we proceeded to look for surface states. The frequencies of surface and defect states are in the ranges of stop bands. In stop bands the right hand side of Eq. 4 is complex and the Bloch wave number k_B takes complex values: $\pm$ j Im(k_B) or $\pi/d \pm$ j Im(k_B) as well [14]. This means that the propagating waves (described by real wave number k_B) are not the solutions in the stop bands and the excitation can be localized on defects (surfaces) with exponential decay of the amplitude: $e^{\pm\gamma}$, where the rate γ= Im(k_B)d is related to imaginary part of propagation constant k_B (see Eq. 3).

To investigate the surface states we considered the equivalent periodic system in the form of infinite sequence of supercells. Each supercell contains two chains composed of n and m networks connected by single network playing the role of defects (surfaces). The surface networks are characterized by parameters q_0 (or C_0) and d_0 which are different from the corresponding parameters q (or C) and d for the networks within the chains. The ABCD matrix for the supercell $\mathbf{M}_{SC}$ can be calculated as a product:

$$\mathbf{M}_{SC} = \boldsymbol{M}_0\boldsymbol{M}^n\boldsymbol{M}_0\boldsymbol{M}^m. \tag{5}$$

Having the matrix $\mathbf{M}_{SC}$, we can obtain the transmission spectrum by calculating S_{21} element of the corresponding scattering matrix [2].

For the larger values of m, $n > 5$ the modes localized at the defected (surface) networks are isolated from each other. We would like to show the effect of frequency selective transmission in the range of frequency gap of MSTL, mediated be surface modes occupying simultaneously both terminations (surfaces) of MSTL. To mimic such behavior in our model we considered two identical defects in one supercell, where the localized excitation is almost spatially isolated by the distance of m networks and coupled in pairs at the smaller distance of n networks ($n<m$).

IV. RESULTS

From numerical calculations performed for MSTL composed of n = 5 identical cells we have got the approximate ranges of first three stop bands: 4.25-8.50 GHz, 11.25-14.75 GHz, 17.75-20.25 GHz. Those results coincide with experimentally measured transmission spectrum where, in the whole accessible frequency range: 8-18 GHz, we found the stop band exactly coinciding with the second stop band. We used this experimentally validated numerical results to fit only two bulk parameters of our lumped-element model: q and ε_{eff}. For q = 24 pF Ω and ε_{eff} = 1.6 (which gives p = 0.178 for d = 16 mm) we have got almost the same ranges of stop bands as for numerical outcomes. In Fig. 2 we showed the dispersion relation for equivalent lumped-element model supplemented by the spectrum of transition through the n = 5 bulk cells (networks) in infinite chain.

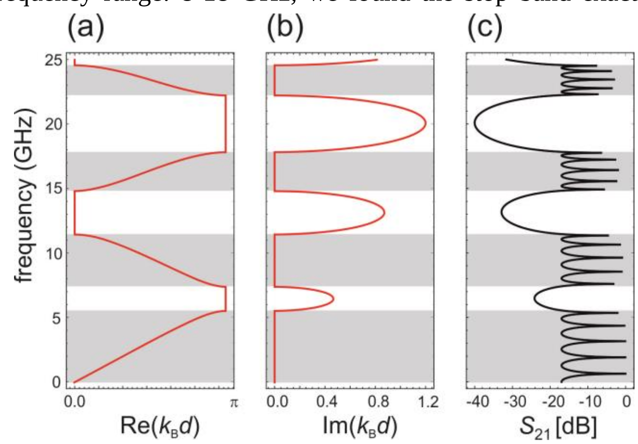

Fig. 2. The dispersion relation (a,b) and transmission spectrum (c) for the equivalent ladder network (see Fig. 1c) equivalent to MSTL. (a,d) The dispersion relation (relation between dimensionless Bloch wave number: $k_B d$ and the frequency) was plotted for infinite ladder composed only with the bulk cells. (c) The S_{21} spectrum was calculated for the transmission trough the n = 5 bulk networks in infinite ladder filter. To match the position of the stop bands of ladder filter to the numerical and experimental spectra, we took the value of parameter: $q = Z_C\, C$ = 24 pF Ω and the effective dielectric constant: ε_{eff}=1.6.

We can see that in the stop bands, where transmission is practically blocked (Fig. 2(c)), the imaginary part of Bloch wave number is non-zero. The condition: Im(k_B) $\neq 0$ ensures the localization of modes in the presence of defects (or surfaces).

Let's discuss now the finite MSTL where the surface states can be observed. In Fig. 3(a) we presented the measured (solid lines) and numerically simulated (dashed lines) transmission spectra for finite MSTL. We considered MSTL composed of n = 5 identical cells (Fig. 1(d)) and MSTL finished by additional cells of different geometry (Fig. 1(b,c)). The transmission spectrum is limited to experimental frequency range 8-18 GHz, covering the second stop band. We can see (the spectra drawn by red lines in Fig. 3(a)), that the presence of terminating cells of altered shape leads to the appearance of surface modes, visible as a sharp doublet of peaks within the stop band. The spatial profiles of out-of-plane components of electric field for those modes are presented in Fig. 3(b,c) at selected time. The modes are localized at the surfaces (terminations) of MSTL and the envelopes of their amplitude decay exponentially inside the structure. The surface modes occupy both surfaces, because the whole structure is symmetric with respect to flipping both ends and there is no mechanism which can preferably select one end for localization. Due to the mirror symmetry one of the surface modes is symmetric (the electric field oscillate in phase on both ends) – see Fig. 3.(b), and the other one – antisymmetric (the electric field oscillates in out-of-phase on both ends) – see Fig. 3(c). For sufficiently large number of cells in the chain the surface modes practically do not penetrate the deep interior of the structure. The field dynamics at one termination of MSTL is then independent on the dynamics on opposite termination. It means that symmetric and antisymmetric surface states will be degenerated in frequency. Such degeneracy makes the experimental detection of surface states difficult. When the MSTL will be driven at one terminal (surface) by the signal of the frequency equal to the frequency of two degenerate surface states, then it will populate both surface states simultaneously. The field barely leaking trough the long structure will be unable to develop its amplitude at opposite terminal (surface) due to destructive interference of symmetric and antisymmetric mode. In our studies we use however MSTL of relatively small number of cells (n = 5 and 7). It ensures the reasonable compromise. We are still able to observe the band structure with the distinctive stop bands but the symmetric and antisymmetric surface states found in the second stop band will have still distinguishable frequencies (about 100 MHz separtion). It allows to transmit the signal in-phase (using symmetric surface state) or with phase flipped (for antisymmetric surface state) between two terminals (surfaces) of MSTL. The signal will be well separated in frequency domain from the modes transmitted in bands below and above stop band.

The effect of geometrical changes of surface cells is reflected in simplified lumped-element model by the change of two (surface) parameters: C_0 (or q_0) and d_0 – see Fig. 1(e). In the studies presented in Fig. 3(d,e) we read out the length d_0 = 0.72 d (directly form the considered geometry of surface cells in MSTL) and we took p_0 = 0.53 p (assuming that the ratio of area of surface cell and bulk cell: S_0/S can by related to appropriate ratio of capacitances: $S_0/S \approx C_0/C \approx p_0/p$). For above values of parameters we found the transmission peak located in the center of the third stop band – see Fig. 3(d). By careful inspection we can notice the peak is doubled. When the number of bulk networks, separating two defected (surface) networks, is lowered then the splitting of doublet is enhanced – see Fig. 3(e). Such behavior is expected for symmetric and antisymmetric surface states found in numerical studies – see Fig. 3(b,c).

We showed that surface states appear in considered system as a result of geometrical changes of the terminal parts of periodic MSTL. We are going to investigate now how to tune the frequencies of surface states within the stop band by adjustment of surface parameters describing the geometry of surface cells of MSTL. We changed length of surface cells d_0 and the width of the wider section in surface cell w_0 (the length of this section l_0 was kept unaltered). We performed the numerical studies where the values of cell w_0 and l_0 were changed gradually. The computations were supplemented by the outcomes obtained from lumped element model, where the change of the parameter w_0 was simulated by the appropriate change of the capacitance C_0 (or parameter q_0).

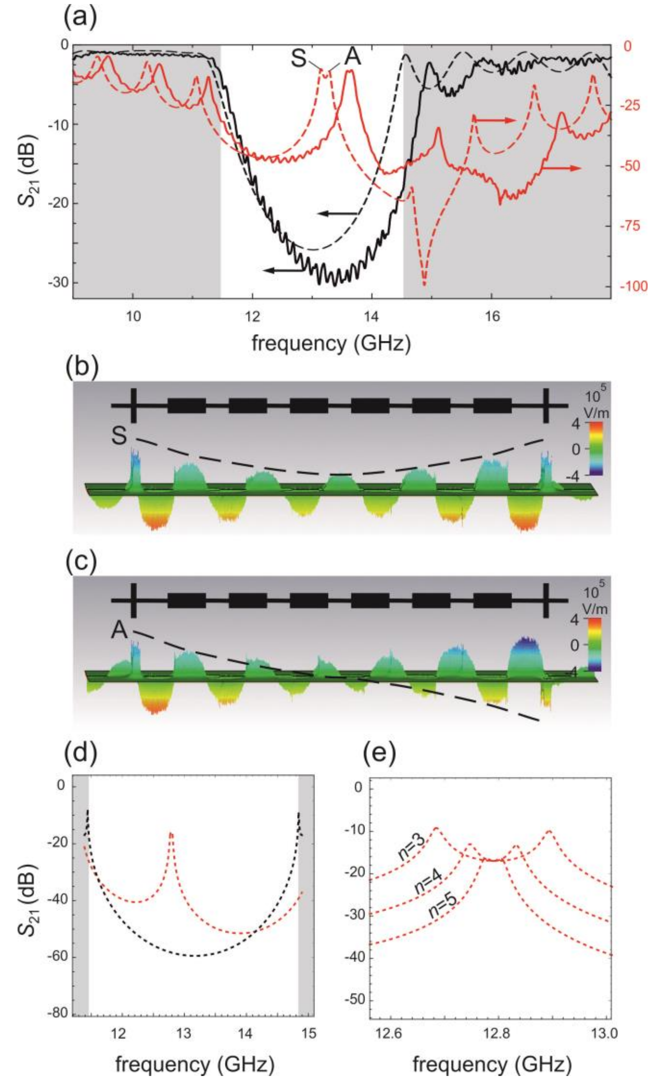

Fig.3. The appearance of the surface states in the second stop band of MSTL. (a) Transmission spectrum S_{21} for MSTL composed of bulk cells n = 5 in the absence of surface cells (black lines), compared to S_{21} spectrum for the same structure completed by surface cells (red lines) – see Fig. 1(a,b). The experimental and numerical data are plotted using solid and dashed lines, respectively. The spatial profiles of (b) symmetric surface state (S) and (c) antisymmetric surface state (A) calculated numerically, corresponding to the doubled of peaks visible in (a). (d) The S_{21} spectrum for lumped element model equivalent to the MSTLs considered in (a) – black (red) dotted line and red dotted line corresponds to the system without (with) surface networks – see Fig. 1(e). For the surface networks we took $d_0 = 0.72d$. and $q_0 = qS_0/S = 0.53q$, where S_0 and S are the areas of the microstripe within the surface cell and bulk cell. (e) The degeneracy of the doubled of surface states is noticeable lifted for shorten sequences of bulk cells.

In Fig. 4 we presented the dependencies of the surface states frequencies on surface parameters: d_0 and w_0 (C_0) in the second stop band of considered MSTL. We used both numerical simulations (Fig. 4(a,b)) and lumped-element model (Fig. 4(c,d)) to investigate those dependencies. Both methods give

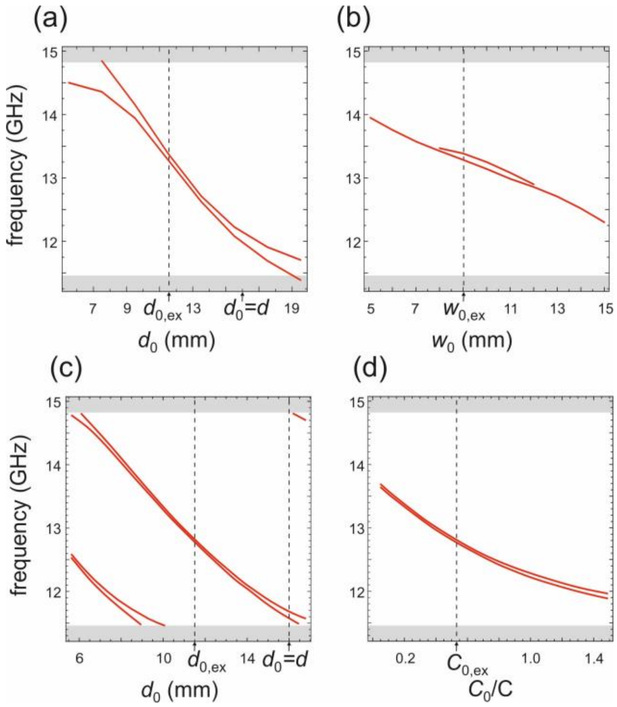

Fig. 4. Tuning the frequency of the surface states by structural changes of the surface cells in the range of the second stop band – for MSTL presented in Fig. 1(a,b). Both for numerical studies (a) and for lumped element model (c) we studied the impact of the length of surface cell d_0 on the frequencies of surface states, where we kept the width of central section of the waveguide w_0 and the capacitance of surface network C_0 unaltered: w_0 = 9 nm (equal to the experimental values $w_{0,ex}$), C_0 = 0.53 C (being the counterpart of the experimental value). For fixed value of d_0 (the same as in the experiment d_0 = 0.73 d) we showed that the frequencies of surface states can be also tuned by adjusting the value of w_0 (in numerical studies – (b)) and C_0 (in the studies based on lumped-element model).

similar results which confirms the applicability of considered lumped element-model for investigation of surface states in periodic MSTL.

By changing the length of surface cell we can shift the doublet of surface states in the whole range of stop band. The lumped-element model predicts that for small values of d_0 an additional doublet of surface states appears at the bottom stop band. However, such states were not found with the aid of numerical simulations in the investigated range of d_0. The doublets tend to split in the vicinity of edges of stop band. This can be explained when we notice that the imaginary part of propagation constant (Bloch wave number) is decreasing in the close to the edges of stop bands (see Fig. 2(b)). Due to that the modes are less localized (see Eq. 3) and the excitation on both terminals of the MSTL can be more correlated to each other. This leads to stronger splitting of the modes which oscillate in-phase (Fig. 3(b)) and out-of-phase (Fig. 3(c)) on both surface.

The frequency of surface states can be also tuned, in considered system, by the change of the width of the central segment in the surface cells w_0 (Fig. 4(b)). The change of the parameter w_0 affects the capacitance of surface cells. Therefore, we changed the capacitance C_0 (and parameter q_0) in lumped element model proportionally to the altered area of surface cells in MSTL (Fig. 4(d)). Such changes of w_0 (or C_0) do not lead,

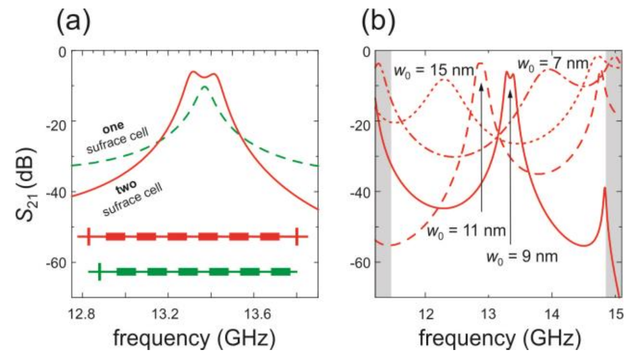

Fig. 5. Presence of surface state doublet in transmission spectrum – numerical studies. (a) Doublet appears only in MSTL width tow identically perturbed surface cells (red curves). When considered MSTL is terminated at one side by surfaces cell of different geometry and at the other side by the cell identical to the bulk cells we observe the single surface state in the spectrum. (b) By changing the surface parameter w_0 (width of the central segment in the surface cells) we can shift the frequency of surface states within the stop gap (see Fig. 4). The splitting of the frequencies (in the vicinity of the edge of stop band) can be accompanied with the broadening of the width of individual peaks in the doublet which can led to merging of two peaks into one (see also Fig.4(b)).

however to the noticeable increase of splitting between symmetric and antisymmetric surface modes when their frequencies are pushed away from the center of stop band. It can be explained by checking how the width of peaks of surface states in transmission spectra changes in dependence on w_0 (see numerical outcomes in Fig. 5(b)). We can notice that when the doublet of peaks is shifted toward the edges of stop band, then the width of peaks increases faster than their separation. As a result peaks forming doublet merge into one wide peak.

For the MSTL terminated asymmetrically, i.e. when the first and the last cell of the structure are not identical, each surface state is localized at one termination only and is manifested in the transmission spectrum as a single peak. The origin of this peak is however different, than the origin of the wide peak resulting from merging to peak doublet described above. In Fig. 5(a) we compared the peak doublet composed of symmetric and antisymmetric surface states (for the structure presented in Fig. 1(a, b) – see also the red sketch in Fig. 5(a)) and the peak of single surface state localized on one surface only (for the structure form Fig. 1(b) with one surface cell omitted – see also the green sketch in Fig. 5(a)). We can notice than the width of the peaks of single surface state is in general much narrower that the width of the merged doublet of symmetric and antisymmetric surface states.

V. CONCLUSION

We investigated experimentally and numerically the surface state in the microwave transmission spectra of the periodic microstripe. We showed that, the frequencies of the surface states can be shifted inside the stop bands by changing the dimensions of elements forming the termination of microstipe. For appropriately adjusted values of these geometrical parameters, the peaks of surface states are splitted into symmetric and antisymmetric surface states, for which the electromagnetic field oscillates on both terminations of the microstripe in-phase or out-of-phase-phase, respectively. These surface modes, which occupy both terminations (surfaces) of periodic microstripe, can be potentially used to transmit the reference signal of selective frequency trough the stop band being well separated from the signals transmitted in the bands.

REFERENCES

[1] J-S. Hong, and M. J. Lancaster, *Microstrip Filters for RF/Microwave Applications*. New York, USA: John Wiley & Sons, Inc, 1998.

[2] D. M. Pozar, *Microwave Engineering*. New Jersey, USA, CA: John Wiley & Sons, Inc., 2011.

[3] J. Guo, Y. Sun, Y. Zhang, H. Li, H. Jiang, and H. Chen, “Experimental investigation of interface states in photonic crystal heterostructures,” *Phys. Rev. E*, vol. 78, pp. 026607, Aug. 2008.

[4] D. P. Belozorov, A. A. Girich, S. V. Nedukh, A. N. Moskaltsova and S. I. Tarapov, “Microwave Analogue of Tamm states in periodic chain-like structures,” PIER Letters, Vol. 46, pp 7-12 (2014).

[5] D. P. Belozorov, A. A. Girich, S. I. Tarapov, “An Analog of Surface Tamn States in Periodic Structures on the Base of Microstrip Waveguides,” *U.R.S.I.(Radio Science Bulletin)*, 345, pp.64-79 (2013).

[6] J. Kłos,” Conditions of Tamm and Shockley state existence in chains of resonant cavities in a photonic crystal,” *Phys. Rev. B*, vol. 76, pp. 165125, Oct. 2007.

[7] I. L. Garanovich, A. A. Sukhorukov, and Y.S. Kivshar, “Defect-Free Surface States in Modulated Photonic Lattices,” *Phys. Rev. Lett.*, vol. 100, pp. 203904, May 2008.

[8] A. P. Vinogradov, A. V. Dorofeenko, S. G. Erokhin, M. Inoue, A. A. Lisyansky, A. M. Merzlikin, and A. B. Granovsky, “Surface state peculiarities in one-dimensional photonic crystal interfaces,“ *Phys.Rev*. B vol. 74, 045128 Jul 2006.

[9] S. I. Tarapov, “Microwaves in dispersive magnetic composite media,” *Low Temp. Phys.*, vol. 38, pp. 603, Jul 2012.

[10] A. Alù and N. Engheta, “Pairing an epsilon-negative slab with a mu-negative slab: resonance, tunneling and transparency,” IEEE Trans. Antennas Propag., vol. 51, pp. 2558-2571, Oct. 2003.

[11] J. Kłos, H. Puszkarski, “Conditions of coexistence of Tamm and Shockley states in a superlattice with a perturbed surface,” Phys. Rev. B, vol. 68, pp. 045316, Jul. 2003.

[12] J. Rychły, J. W. Kłos, “Spin wave surface states in 1D planar magnonic crystals,” *J. Phys. D : Appl. Phys*., vol. 50, pp. 164004, Mar. 2017.

[13] L. Tong, B. M. Sadler, M. Dong, “Pilot-assisted wireless transmissions: general model, design criteria, and signal processing,” IEEE Signal Process Mag. vol. 21, pp. 12 – 25, Nov. 2004.

[14] N. W. Ashcroft, N. D. Mermin, *Solid State Physics*. Orlando, USA: Harcourt, Inc. 1976.

Aleksey A. Girich (M’10-M’12) was born in Kharkov, Ukraine. He obtained his MS degree in Lasers and Electro-Optics from the Kharkov National University of Radioelectronics (KNURE) in 2005 and PhD degree in Radiophysics from the KNURE in 2013.

Since 2006, he has been a Member of the Research Staff at the IRE NASU. Currently he is a senior scientist with the Department of Radiospectroscopy, IRE NASU, Kharkov, Ukraine. His research interests include photonic crystals, surface waves in structures on basis of photonic crystals, metamaterials, magnetic nanostructures, magnetic properties of multilayer systems, magnetic resonance, disc dielectric resonators. He is the author and co-author of over 50 journal and conference papers.

Anna A. Kharchenko (M’09-M’13) was born in Kharkov, Ukraine. She got her MS degree in 2008 at the Faculty of Applied Mathematics and Management of Kharkov National University of Radioelectronics.

Since 2007, she has been an active young scientist of the Research Staff at the IRE NASU. In 2014 she successfully defended her postgraduate thesis in radiophysics and in 2015 she got her Ph.D. Her research interests include magnetic/nonmagnetic periodic and multiperiodic structures, surface waves in structures on basis of periodic structures, metamaterials, nanostructures, magnetic properties of multilayer systems, magnetic resonance. She is the author and co-author of over 30 journal and conference papers.

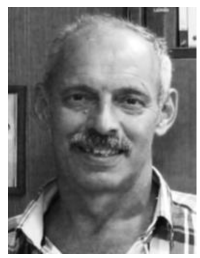

Sergey I. Tarapov was born in Kharkov, Ukraine at 02.09.1954. He graduated from Kharkov State University in 1976. PhD in Phys and Math - 1987. Dr. in Phys and Math - 1994. Corresponding member of National Academy of Ukraine - 2015. Chief of Dept. In Institute of Radiophysics and Electronics (IRE NASU).

His main scientific interests belong to experimental study in: physics of metamaterials, magnetic spectroscopy of nanostructured magnets; low-temperature physics; extra-high frequency electronics. He is an author of about 390 publications.

Szymon Mieszczak finished master studies in 2017 and has started PhD at Adam Mickiewicz University.

His main research area is spin waves dynamics in magnonic crystals and quasicrystals

Jarosław W. Kłos. (M’17) was born in 1975 in Poznan, Poland. He graduated and obtained PhD in physics (2005) at Adam Mickiewicz University in Poznan.

His current research area is spin waves dynamics in magnonic crystals. He is an author over 50 publications.

Maciej Krawczyk was born in 1971. He graduated and obtained PhD in physics (2001) at Adam Mickiewicz University in Poznan, he is a full-professor since 2015.

His current research area is spin waves dynamics in magnonic crystals and skyrmions. He is an author over 110 publications.